

Nonlinear interactions of spin waves with parametric pumping in permalloy metal films

G. A. Melkov, Yu. V. Koblyanskiy, R. A. Slipets, and A. V. Talalaevskij
Faculty of Radiophysics, Kiev National Taras Shevchenko University, 01033 Kiev, Ukraine

A. N. Slavin

Department of Physics, Oakland University, Rochester, Michigan 48309-4401, USA

(Received 22 October 2008; revised manuscript received 13 February 2009; published 8 April 2009)

Nonlinear interactions of dipolar and dipole-exchange spin waves with microwave magnetic field of parametric electromagnetic pumping were studied experimentally in thin permalloy (Py) films. It was demonstrated that parametric pumping in Py films leads to efficient amplification of the “trace” of quasistanding spin waves created due to the two-magnon scattering by the input signal pulse of long-wavelength dipolar spin waves and, then, to suppression of the amplified signal due to the parametric excitation of short-wavelength exchange-dominated spin waves. It was, also, shown that nonlinear interactions of spin waves in Py films can be used for the development of microwave signal processing devices and for the measurement of relaxation characteristics of different spin-wave groups.

DOI: [10.1103/PhysRevB.79.134411](https://doi.org/10.1103/PhysRevB.79.134411)

PACS number(s): 75.30.Ds, 76.50.+g, 85.70.Ge

I. INTRODUCTION

Nonlinear interactions of spin waves in magnetic films are studied intensively because they are responsible for such fundamentally interesting nonlinear phenomena as wave-front reversal in a three-wave parametric process,¹ reversal of magnetic relaxation,² and storage and parametrically stimulated recovery of microwave signals.³ At the same time, the investigations of the nonlinear wave interactions in magnetic films can lead to the development of passive and active nonlinear microwave signal processing devices capable of performing such useful operations as controlled signal delay, signal amplification, reversal of the signal time profile, enhancement of the signal-to-noise ratio, and reception of microwave signals on noisy background when signal amplitude is well below the noise level.^{4–7}

Most of the spin-wave microwave signal processing devices, existing today, are based on ferrite films made from the yttrium iron garnet (YIG).^{1–7} Although YIG as a material for microwave technology has a major advantage of a record low ferromagnetic resonance (FMR) linewidth ($\Delta H \leq 0.5$ Oe, relaxation time $\tau \geq 0.2$ μ s), the practical applications of the YIG-based devices are limited due to several important drawbacks of YIG, such as relatively low static magnetization and, therefore, relatively large magnitude of the bias magnetic field necessary for the device operation in the microwave and especially in the millimeter frequency band, low temperature stability of the device characteristics related to the relatively low Curie temperature of YIG, and relatively large size of elements of typical etch patterns in YIG, which is of the order of several micrometers.

Most of these drawbacks can be eliminated by using metallic [e.g., permalloy (Py)] magnetic films. Unfortunately, the direct replacement of YIG by permalloy in standard microwave devices, for example, in passive spin-wave delay lines,⁸ is not possible because the spin-wave propagation losses in permalloy are almost 100 times larger than in YIG due to the much larger FMR linewidth in permalloy ($\Delta H \cong 25–50$ Oe). Due to this rather large FMR linewidth the dipolar spin waves [or magnetostatic spin waves (MSWs)] in

permalloy are practically nonpropagating as they decay aperiodically very close to the input antenna. The typical mean free path of dipolar spin waves in permalloy does not exceed several tens of microns and the typical relaxation time τ_k of these waves is rather short, of the order of 1–2 ns.

It is possible to overcome this difficulty by using the phenomenon of spin-wave amplification and restoration by the external parametric pumping, similar to the one observed in Ref. 3 in ferrite YIG films. In this process a microwave signal of the frequency ω_s , supplied to the input antenna excites in a permalloy film a fast dipolar spin wave [or surface magnetostatic spin wave (SMSW)] with the wave number $k_s \leq 10^2$ cm^{-1} and group velocity $v_g \sim 10^7$ cm/s . Because of a considerable damping in permalloy this wave propagates from the input antenna only for several tens of microns. In the process of this short-distance propagation, mostly due to the two-magnon scattering,^{8,9} the SMSWs are partly transformed into a different type of dipolar spin waves—the backward volume magnetostatic spin waves (BVMSWs). These BVMSWs are quasistanding, as they have a very low group velocity ($v_g \sim 0$) and a typical wave number $k_B \sim 10^4$ cm^{-1} , and they exist in the same small region (of the order of several tens of microns) near the input antenna, where the signal-induced SMSWs were propagating.³

Basically, we can say that these quasistanding BVMSWs form a “trail” along the path of the propagating and decaying SMSW pulse excited by the input microwave signal. If now, during the time interval when the amplitudes of “trail-forming” BVMSW are still well above the thermal noise level, we apply a pulse of microwave pumping having carrier frequency ω_p which is twice larger than the signal carrier frequency ω_s ($\omega_p = 2\omega_s$), we can get a substantial frequency-selective parametric amplification of the BVMSW with frequencies $\omega_k \sim \omega_s = \omega_p/2$.^{1–6,10–12} This parametric *parallel* pumping, in which the microwave magnetic field of the pumping is parallel to the direction of the in-plane bias magnetic field, leads, also, the wave-front reversal of BVMSW and conversion of quasistanding BVMSW back into the SMSW propagating *towards the input antenna*, where they are converted into a delayed electromagnetic output signal,

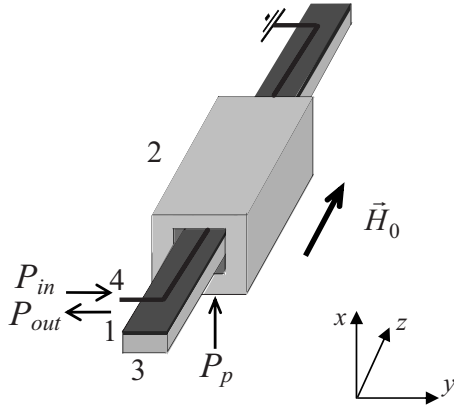


FIG. 1. Experimental set-up: 1—permalloy (Py) film, 2—pumping open dielectric resonator, 3—dielectric substrate, 4—wire antenna, P_p —pumping power, P_{in} —power of the input signal, P_{out} —power of the output restored signal, and H_0 —bias magnetic field.

which we will call below a *restored* signal, following Refs. 2 and 3.

The amplitude, the duration, and the time delay of the output restored signal are determined by the time interval T_p between the leading front of the input pulse and the leading front of the pumping pulse, the power P_p , and the duration τ_p of the pumping pulse. The shape of the restored output signal is influenced, also, by the another (third) spin-wave group—the group of so-called *parametric* spin waves (PSWs) with $k_p > 10^5 \text{ cm}^{-1}$, which are excited by parametric pumping and increase from the thermal level when the pumping is applied. When the amplitudes of PSWs become comparable to the amplitudes of SMSWs and BVMSWs, created by the coherent input microwave signal, PSWs start to interact nonlinearly with SMSWs and BVMSWs and this interaction leads to the suppression of parametric amplification of SMSWs and BVMSWs, and, essentially to the decrease in the amplitude of the restored output signal.³ This suppression effect finds a natural explanation in the framework of the self-consistent theory of parametric interaction of spin waves (S-theory).¹⁰

II. EXPERIMENTAL SETUP AND RESULTS

The experimental investigations of the parametric interaction of a pumping pulse having carrier frequency ω_p with input microwave pulse of the carrier frequency $\omega_s = \omega_p/2$ in a permalloy (77%—Ni, 23%—Fe, saturation magnetization $4\pi M_0 = 10.6 \text{ kG s}$) film were performed at the experimental setup shown in Fig. 1. The Py film waveguide deposited on a silica substrate had the dimensions of $0.5 \mu\text{m} \times 1.6 \text{ mm} \times 20 \text{ mm}$ and was placed inside a rectangular opening in the open dielectric resonator (ODR) made of thermostable ceramics with dielectric permittivity $\epsilon \cong 80$. The microwave magnetic field of the ODR was parallel to the bias magnetic field H_0 , i.e., the case of parallel parametric pumping (see Chap. 10 in Ref. 8) was realized in our experiment. The microwave pumping pulses of the carrier frequency $f_p = \omega_p/2\pi = 9.4 \text{ GHz}$, duration τ_p varied in the interval

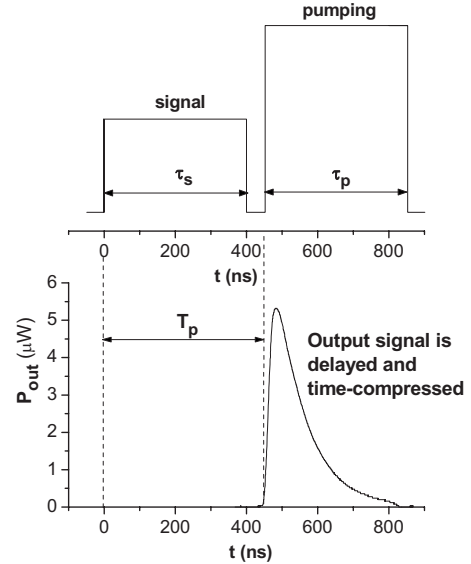


FIG. 2. Upper frame: relative temporal positions of the input signal pulse and pumping pulse. Lower frame: typical profile of the envelope of the restored output microwave signal measured in a Py film for the following parameters: signal power $P_s = 2 \text{ mW}$, $\tau_s = 400 \text{ ns}$, pumping power $P_p = 120 \text{ W}$, $\tau_p = 400 \text{ ns}$, $T_p = 400 \text{ ns}$, and $H_0 = 260 \text{ Oe}$.

$10 \text{ ns} \leq \tau_p \leq 400 \text{ ns}$, and power P_p varied in the interval $0 < P_p < 125 \text{ W}$ (21 dBW) were supplied to the pumping ODR. The wire antenna of the diameter $d = 50 \mu\text{m}$ placed on the Py film was used for the excitation and reception of fast SMSW. The SMSW wave packets, excited by the input electromagnetic signal of the carrier frequency $f_s = 4.7 \text{ GHz}$, duration varied in the interval $10 \text{ ns} < \tau_s < 400 \text{ ns}$, and power of $P_s \leq -27 \text{ dBW}$, were propagating perpendicular to the direction of the in-plane bias magnetic field.

As it was mentioned above, both the signal-induced SMSW and the quasistanding BVMSW, excited as a result of two-magnon scattering of SMSWs on the film defects and forming a “trail” of the propagating SMSW wave packet, had significant amplitudes only in the immediate vicinity of the input wire antenna. When the pumping pulse was supplied to the pumping ODR the BVMSWs were amplified and phase conjugated. Thus, due to the inverse two-magnon scattering they formed a SMSW packet propagating back to the input antenna, where this packet was converted into the restored and delayed output electromagnetic signal. While the propagating SMSW could interact with the input antenna directly, the signal from quasistanding BVMSW was caused by the reverse two-magnon conversion of these waves into SMSW.

A typical wave form of the restored and delayed output signal is shown in Fig. 2. This output pulse profile was obtained for the input signal pulse of the duration $\tau_s = 400 \text{ ns}$ and power $P_s = 2 \text{ mW}$, pumping pulse of the duration $\tau_p = 400 \text{ ns}$ and power $P_p = 120 \text{ W}$, and the pumping delay time T_p that was larger than the duration of the signal pulse $T_p \geq \tau_s$. In general, the properties of the restored output pulse obtained on a Py film (see Fig. 2) were similar to the properties of the analogous restored pulse obtained in a ferrite YIG film.³ Namely, the restored signal existed only during

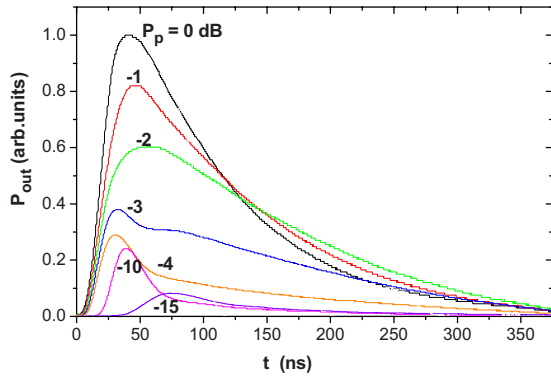


FIG. 3. (Color online) The temporal profile of the output restored signal for different pumping powers P_p (dB) (0 dB corresponds to $P_p=120$ W). The time $t=0$ corresponds to the moment when pumping pulse was switched on ($t=T_p$ in Fig. 2). All the other parameters are the same as in Fig. 2.

the time interval when the pumping was switched on, it had a bell-like shape and duration that was independent of the input pulse duration τ_s , the amplitude of this pulse was increasing with the increase in τ_s , and the slope of the leading front of the restored pulse was increasing with the increase in the pumping power P_p .

In spite of these similarities there were, also, significant differences in the parametric signal restoration process observed in Py film compared to the case of a YIG film.³ These differences were caused by the fact that the spin-wave relaxation time τ_k in Py is 2 orders of magnitude shorter than in YIG and by peculiarities of the spin-wave spectrum in Py films.

The evolution of the shape of the output restored signal P_{out} with the increase in the pumping power P_p is shown in Fig. 3. For relatively small pumping powers $-15 \text{ dB} \leq P_p \leq -4 \text{ dB}$, similar to the case of the YIG film,³ with the increase in the pumping power P_p , the profile of the output restored signal becomes narrower and the delay time before its appearance is reduced. It is obvious from Fig. 3 that the temporal position of the maximum of the output restored signal, characterized by the delay time T_d from the leading front of the pumping pulse, is changing from ~ 70 ns for $P_p=-15$ dB to ~ 25 ns for $P_p=-4$ dB. Note that for the case of a YIG film similar delay times were 2 orders of magnitude larger and reached several microseconds.³

When the pumping power was increased over -4 dB (see the trace corresponding to $P_p=-3$ dB in Fig. 3) a second maximum appears in the profile of the output restored pulse. This second maximum becomes dominant for $P_p \geq -2$ dB. The evolution of the second peak with the further increase in the pumping power is qualitatively similar to the evolution of the first peak (and to the evolution of the restored signal in YIG films): the output signal profile becomes narrower and the time delay T_d of its maximum is decreased. The dependences of the output signal width Δt (at half-maximum power) and the time delay of its maximum T_d as functions of the pumping power P_p are shown in Figs. 4(a) and 4(b), respectively. It is clear from Fig. 4 that there is a jump in both these quantities at $P_p=-4$ dB, corresponding to the appearance of the second peak in the output signal profile.

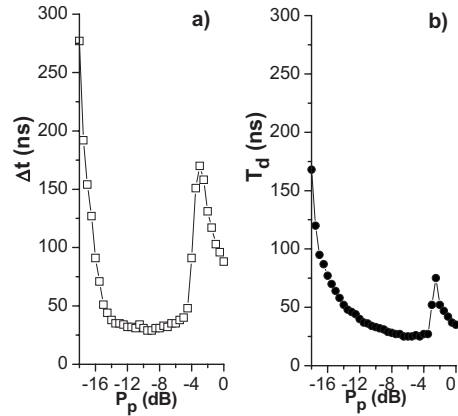


FIG. 4. Dependences of the parameters of the restored output signal on the pumping power P_p : (a) width Δt (at the half-power level); (b) temporal position of the signal maximum T_d relative to the moment when the pumping was switched on. All the other parameters are the same as in Figs. 2 and 3.

It is obvious from Fig. 3 that during the action of the pumping pulse the output restored signal, after reaching a maximum at $t=T_d$, begins to fall exponentially $P_{out} \sim \exp(-\tau_{kp}t)$ for $t > T_d$ with a characteristic relaxation time $\tau_{kp} > \tau_k$, which is dependent on the pumping power P_p . We believe that this exponential decrease results from the fact that the amplitude of the effective parametric pumping acting on the quasistanding BVMSW is reduced below the threshold level necessary for parametric amplification because of the nonlinear interaction of pumping with PSWs excited by pumping from the thermal level (see S-theory in Ref. 10 for the detailed explanation of this interaction mechanism). For example, for $P_p=0$ dB (120 W) the output restored signal reaches a maximum at $t=T_d=40$ ns and the relaxation time of the output signal for $t > T_d$ is $\tau_{kp} \sim 200$ ns. This value of the relaxation time characterizes the lifetime of MSW in the presence of pumping of a given magnitude ($P_p=120$ W in this case) in a steady state. It is obvious that in the transient period ($t > T_d$), when the pumping has already started to act and before the spurious influence of PSW started to manifest itself, the relaxation parameter of the MSW is negative, and, therefore, the amplitude of the output signal exponentially increases with time. It is worth noting that the relaxation time τ_{kp} of MSW in a Py film in the presence of parametric pumping can be made to be equal to (or of same order of magnitude as) the relaxation time of MSW in YIG films without pumping. Thus, there is a real possibility to use active (pumped) devices based on Py films in microwave signal processing.

As we can see from Fig. 3, if the pumping pulse is sufficiently long, the restored signal up to the times $t \sim 400$ ns decreases monotonously and exponentially almost to the noise level. If, on the other hand, we turn off the pumping before this time ($\tau_p < 400$ ns), when the restored signal is still large, the sharp decrease in the restored signal is observed for $t > \tau_p$. This behavior is clearly seen in Fig. 5, where the profiles of the output restored signals, obtained for $P_p=0$ dB (120 W) and different pumping pulse durations τ_p , are shown. In all cases for $t > \tau_p$, i.e., after the pumping has

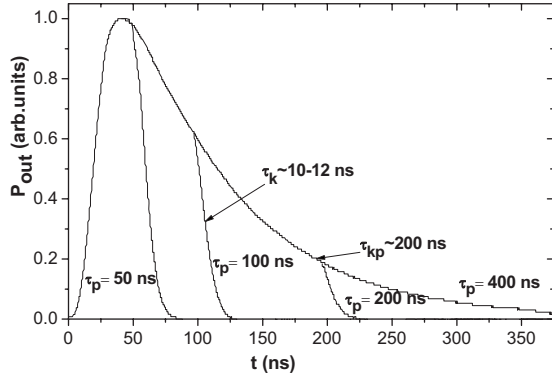


FIG. 5. The temporal profile of the output restored signal for different durations of the pumping pulse $\tau_p=50, 100, 200,$ and 400 ns. $P_p=0$ dB (120 W) and all the other parameters are the same as in Figs. 2 and 3.

been turned off, the exponential decay of the output signal, characterized by the relaxation time τ_k , becomes much faster than in the presence of pumping. For the case presented in Fig. 5 this relaxation time is equal to $\tau_k=10-12$ ns; we have every reason to believe that this time characterizes the intrinsic MSW lifetime in a Py film without the damping-compensating influence of the pumping. We note once again that this intrinsic MSW relaxation time τ_k in Py is at least one order of magnitude shorter than the pumping-enhanced MSW relaxation time $\tau_{kp} \sim 200$ ns.

The dependence of the peak power of the restored output signal on the magnitude of the external in-plane bias magnetic field H_0 is shown in Fig. 6. This dependence has a resonance form with a maximum near the value of $H_0=260$ Oe, which is approximately 12 Oe lower than the field of FMR in a Py film at the signal frequency $f_s=f_p/2$

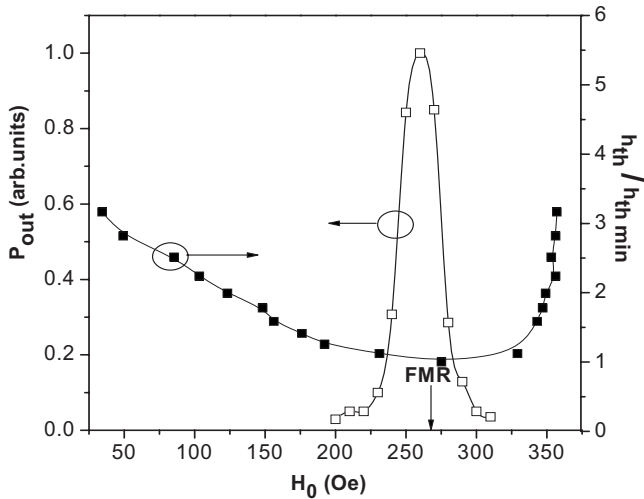


FIG. 6. Dependence of the power P_{out} (□) of the output restored signal on the bias magnetic field H_0 for $\tau_s=\tau_p=400$ ns, $P_s=2$ mW, and $P_p=0$ dB (120 W). The solid squares (■) show the dependence of the normalized $[h_{th\ min}=(20 \pm 5)$ Oe at pumping power $P_p=-18$ dB] parallel pumping threshold $h_{th}/h_{th\ min}$ on the bias magnetic field measured in Py film for the pumping pulse duration $\tau_p=10$ μ s. The arrow \downarrow indicates the bias magnetic field corresponding to the FMR in a Py film.

$=4672$ MHz. The FMR field at the frequency f_s ($H_0=H_{res}=272$ Oe) was measured by finding the minimum of the signal reflection from a short-circuited input antenna 4 (see Fig. 1) when the bias magnetic field was varied. The FMR linewidth in the experimental Py film in these measurements was found to be $\Delta H_0=45$ Oe. We note that the measured linewidth of the restored signal, according to Fig. 6, turns out to be smaller: $\delta H_0=33$ Oe.

To show the position of the bias magnetic field range, where the pumping-induced signal restoration process takes place, relative to spin-wave spectrum of the experimental Py film we present in Fig. 6 experimentally measured magnetic field dependence of the threshold field h_{th} of parametric instability under parallel pumping (or so-called “butterfly” curve⁸). This curve is measured for the duration of the pumping pulse equal to $\tau_p=10$ μ s. The threshold was determined through the appearance of distortions in the envelope of the pumping pulse which was reflected from the open dielectric resonator containing the Py film. Below the threshold this reflected pumping pulse (as well as the incident pumping pulse) had a rectangular shape. Immediately above the threshold the characteristic distortions¹³ appeared near the trailing front of the reflected pulse. These distortions are caused by the parametric excitation of spin waves that exponentially grow with time and create additional losses in the pumping circuit.^{8,13}

The instability threshold has a minimum $h_{th}=h_{th\ min}$ near the FMR field $H_{res}=272$ Oe. To find the absolute value of this threshold we, first, measured a spin-wave instability threshold field of a monocrystalline YIG sphere (of the diameter $d=1$ mm) when the sphere was placed inside a rectangular cavity resonator of the oscillation mode H_{102} . Then, with the help of the ODR, which was used in our current experiment (see 2 in Fig. 1), the instability thresholds of the monocrystalline sphere and the studied Py film were compared. Thus, the value of the instability threshold in a Py film equal to $h_{th\ min}=(20 \pm 5)$ Oe was obtained. This value of the parametric instability threshold corresponds to the intrinsic spin-wave lifetime (determined from the threshold) of $\tau_{k\ th} \sim 2$ ns. It is important to note that the shape of the threshold curve in Py film, presented in Fig. 6, looks similar to monotonous butterfly curves, characteristic for bulk magnetic samples, and is rather different from the butterfly curve in thin (thickness $L \sim 0.5$ μ m) YIG films,⁸ where successive excitation of thickness modes of spin-wave resonances with the increase in the bias magnetic field results in a complicated nonmonotonous behavior of the butterfly curve.^{8,13} Another characteristic feature of the butterfly curve, experimentally measured in a Py film, is the sharp increase in the threshold field for $H_0 > 325$ Oe.

In our experiments performed on a Py film we, also, found a rather unusual dependence of the power of the restored output signal on the delay time T_p between the leading front of the pumping pulse and the leading front of the input signal pulse (see Fig. 2). It turned out that the effect of pumping-induced signal restoration takes place only in a certain interval of the time delays T_p , which we decided to call an *active* interval. The maximum of the restored signal in our experiments was observed *only* when the signal pulse was switched on *earlier* than the pumping pulse, i.e., when the

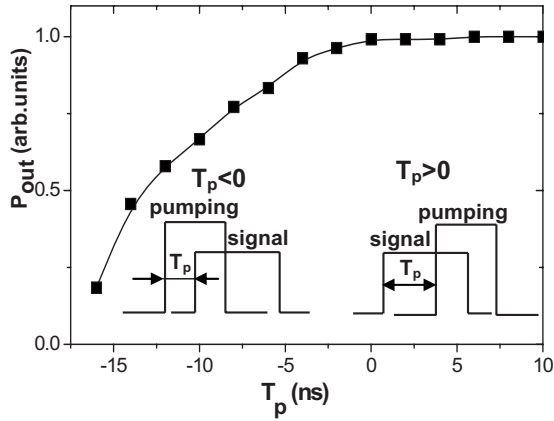


FIG. 7. Dependence of the power P_{out} of the restored output signal on the time delay T_p between the leading front of the pumping pulse and the leading edge of the signal pulse (see, also, Fig. 2). The interval where $T_p < 0$ corresponds to the situation when the pumping pulse is supplied before the signal pulse (see insets at the bottom of the figure).

time delay between the signal and pumping pulses was positive $T_p > 0$.

If, on the other hand, the signal pulse was switched on at least 20 ns later than the beginning of the pumping pulse ($T_p < -20$ ns) than for any durations τ_s and τ_p of the signal and pumping pulses the process of pumping-induced signal restoration did not happen.

Figure 7 demonstrates the experimental dependence of the power P_{out} of the output restored signal on the time delay T_p of the pumping pulse. It is obvious from Fig. 7, that in the case when pumping was switched on after the beginning of the signal pulse ($T_p > 0$), the power of the output restored signal P_{out} was practically independent of T_p . In contrast, when the pumping power was switched on *before* the beginning of the signal pulse ($T_p \leq -5$ ns) P_{out} decreased noticeably at $T_p = -16$ ns it was reduced by 80% and at $T_p \leq -20$ ns no noticeable power of the restored signal was registered.

III. DISCUSSION OF THE RESULTS

All the above described experimental results can be explained on the basis of the theory of microwave signal restoration induced by parametric pumping,³ taking into account the peculiarities the spin-wave spectrum of the studied Py film. The restoration theory³ is based on the assumption that several different groups of spin waves are excited in a magnetic sample.

Below, we shall consider three different groups of spin waves: SW_1 , SW_2 , and SW_3 . Each of these groups is characterized, first of all, by the magnitude of its coupling to the signal-induced microwave magnetic field of the input antenna and, also, by different amplitudes a_1, a_2, a_3 . Let us assume that at the moment when the pumping pulse is switched on [i.e., at the time $t = T_p$ (see Fig. 2)], the initial wave amplitudes are such that $a_{10} > a_{20} > a_{30}$, i.e., the waves of the second group interact with the antenna stronger than the waves of the third group but weaker than the waves of

the first group. We shall, also, assume that due to the radiation loss, caused by interaction with the input antenna, the waves of the first group will have the highest threshold of parametric excitation h_{th} , while the similar threshold will be the lowest for the waves of the third group: $h_{\text{th1}} > h_{\text{th2}} > h_{\text{th3}}$.

When the power P_p of the pumping pulse is increased, so that $h_p > h_{\text{th3}}$, the amplitudes of the third spin-wave group SW_3 , having the lowest threshold of parametric instability, start to grow exponentially with time when $t > T_p$. Due to the weak coupling with antenna this spin-wave group does not contribute significantly to the output signal. With the further increase in pumping, in particular when $h > h_{\text{th2}}$, the amplitudes of the second spin-wave group SW_2 start to increase exponentially with time when $t > T_p$ along with the amplitudes of the third group SW_3 . Due to the larger initial amplitude $a_{20} > a_{30}$ during a certain time interval of the pumping action the second spin-wave group SW_2 will be dominant, and this second group will mainly form the output signal at the antenna. However, due to the fact that the third spin-wave group SW_3 has a larger increment of parametric amplification than the second group SW_2 , with time the amplitudes a_3 will increase faster than the amplitudes a_2 ; the third spin-wave group SW_3 will become dominant again. As a result of this dominance the effective pumping for the second spin-wave group SW_2 will fall below the critical level and the amplitude a_2 will start to decrease exponentially as $\sim \exp(-t/\tau_{kp})$. Therefore, the restored and delayed output signal caused by the second spin-wave group SW_2 will have a form of a pulse with exponentially increasing leading front and exponentially decreasing trailing front.

It was shown in Ref. 3 that under the influence of a powerful pumping the time delay T_d of the maximum of output restored signal and the width of this maximum Δt at half-power level are decreasing with the increase in the amplitude of the pumping field h_p ,

$$T_d \sim h_p^{-1}, \quad \Delta t \sim h_p^{-1}. \quad (1)$$

A similar situation occurs for $h > h_{\text{th1}}$ with the first spin-wave group SW_1 , which, at first, grows exponentially, becomes dominant, and forms the output signal due to its larger initial amplitude, and, then, with time, is suppressed by the third spin-wave group SW_3 , which has the largest increment of parametric amplification. The parameters of the output pulse, caused by the first spin-wave group SW_1 , also, satisfy the conditions [Eq. (1)].

As it was mentioned above, the waves belonging to the third group SW_3 have the lowest threshold of parametric excitation. Only the waves of this type exist in the stationary regime of parametric pumping, i.e., in the case when the pumping pulse duration τ_p substantially exceeds all the relaxation times of the spin system in a magnetic film. The spin waves in the group SW_3 have large magnitudes of the wave vector $k \geq 10^5 \text{ cm}^{-1}$. As a result, they practically do not interact with the microwave magnetic field of the antenna and under the influence of the parametric pumping they grow from the thermal level a_T ($a_{30} = a_T$). It is due to the parametric excitation of these short-wavelength spin-wave group characteristic distortions¹³ which appears in the shape of the

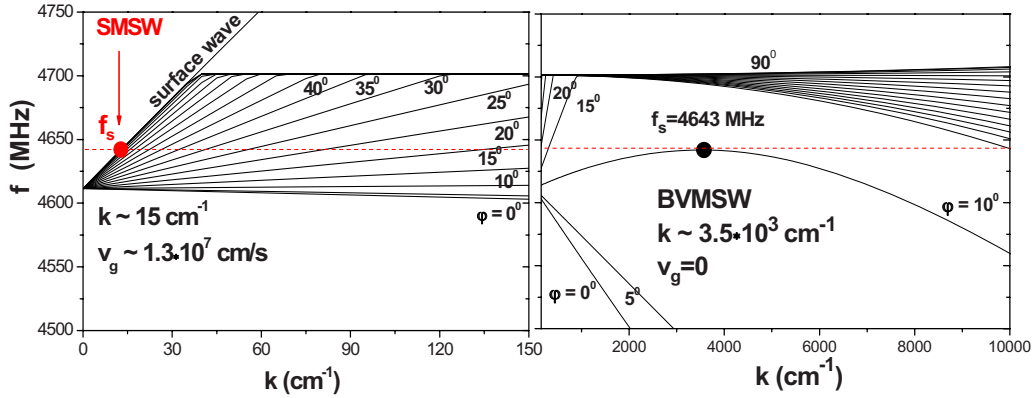


FIG. 8. (Color online) Dipole-exchange spin-wave spectrum of the two lowest thickness modes ($n=0$ and $n=1$), propagating at the angle φ to the direction of the in-plane bias magnetic field \mathbf{H}_0 in a permalloy film with unpinned surface spins. The spectrum was calculated using Ref. 15 for the following parameters: film thickness $L=0.5 \mu\text{m}$, bias magnetic field $H_0=260 \text{ Oe}$, saturation magnetization $4\pi M_0=10.6 \text{ kG s}$, and exchange constant $\alpha=A/2\pi M_0^2=2.3 \times 10^{-13} \text{ cm}^2$. The curves were calculated with the angle φ interval of 5° .

pumping pulse reflected from the magnetic sample in the traditional “parallel pumping” experiments, and the standard method of measurement of parametric instability threshold is based on the registration of these distortions in the shape of the reflected pumping pulse.^{8,13} Although the waves of the group SW_3 have rather large amplitudes, due to their negligible coupling to the antenna, these waves do not contribute to the restored output signal, and their main role is in the renormalization of the amplitude of effective parametric pumping for the first two spin-wave groups, leading to the eventual suppression of the spin-wave groups SW_1 and SW_2 .

The above described model of the spin-wave interaction with parametric pumping allows us to provide a qualitative explanation of the experimental results presented in Figs. 3 and 4. When the pumping power is relatively small $P_p < -4 \text{ dB}$ the restored output signal is formed by the second spin-wave group SW_2 . With the increase in the pumping power P_p the maximum in the output signal profile increases and shifts to the smaller values of delay time T_d , in accordance to relation (1). It is clear from Figs. 3 and 4(b) that for $P_p = -17 \text{ dB}$, $T_d = 170 \text{ ns}$, while for $P_p \leq -4 \text{ dB}$, $T_d = 25 \text{ ns}$. The width Δt of the maximum in the output restored signal is, also, reduced with the increase in P_p in accordance with Eq. (1) [see Fig. 4(a)]. Then, starting from the pumping power $P_p > -4 \text{ dB}$ (see Figs. 3 and 4) the second maximum appears on the profile of the output restored signal at the delay time $T_d = 75 \text{ ns}$, and this second maximum, created by the first spin-wave group SW_1 , becomes dominant with the further increase in the pumping power. Similar to the first maximum, the width Δt and the delay time T_d of the second maximum decrease with the increase in the pumping power $P_p > -4 \text{ dB}$.

We would like to stress again that the decrease in the amplitude of the output restored signal at $t > T_d$ is caused by the spurious influence of the third group of spin waves SW_3 on the parametric amplification of the spin-wave groups SW_1 and SW_2 by pumping. Because of the large value of their wave number, the waves in the SW_3 group do not contribute directly to the formation of the output signal at the antenna. It is, however, obvious from Fig. 3 that with the increase in the pumping power, and, therefore, with the increase in am-

plitudes in the SW_3 group, for $t > T_d$ the rate of the exponential decrease in the output restored signal created by spin-wave groups SW_1 and SW_2 increases significantly.

As it was explained earlier, the sharp decrease in the output restored signal after the parametric pumping has been switched off (see Fig. 5 for $t \geq \tau_p$) is determined by the intrinsic dissipation of the spin-wave amplitude in Py. The experimentally measured intrinsic relaxation time in Py, $\tau_k = 10\text{--}12 \text{ ns}$, determined from Fig. 5, turned out to be about five times larger than the value of the spin-wave relaxation time $\tau_{k \text{ th}}$, determined by measuring the spin-wave instability threshold (see Fig. 6). Here we have no other choice but to conclude that one of the methods used to measure the intrinsic relaxation time in Py is incorrect. Most probably, it is the method of determination of the spin-wave relaxation time from the measurements of the threshold field of parallel pumping instability. This method was developed for dielectric (ferrite) samples, and, therefore, it does not take into account the fact that in metallic films formation of uniform inductive currents could significantly decrease the magnitude of the effective microwave pumping field acting in the film.

It would be interesting and important to determine what spin waves existing in Py film could play the roles of the above discussed spin-wave groups SW_1 , SW_2 , and SW_3 . To solve this problem we calculated the dipole-exchange spin-wave spectrum of the Py film used in our experiment, assuming that the surface spins at the film boundaries are unpinned. This spectrum for the lowest thickness spin-wave mode, propagating at the angle φ to the direction of the in-plane bias magnetic field \mathbf{H}_0 , calculated using the formalism^{14,15} is presented in Fig. 8. In this spectrum the waves propagating along the direction of the bias magnetic field \mathbf{H}_0 ($\varphi=0$) are the BVMSWs having uniform distribution of the variable magnetization along the film thickness ($n=0$). The minimum frequency of these waves for the conditions of our current experiment is $f_{0 \text{ min}} = 1680 \text{ MHz}$ [not shown in Fig. 8] and corresponds to the wave vector magnitude of $k = 2 \times 10^5 \text{ cm}^{-1}$. This point, also, corresponds to the bottom of the spin-wave spectrum of the in-plane magnetized Py film. For $\varphi \geq 15^\circ$ the volume waves are transformed into the quasi-surface MSWs, having exponential distribution of the vari-

able magnetization along the film thickness [although for low values of the in-plane wave number k this distribution is close to the uniform one ($n=0$)].¹⁴ With the increase in the in-plane wave number k the ($n=0$) surface wave is hybridized with a similar mode having one node ($n=1$) in its magnetization distribution along the film thickness (this thickness distribution is close to the first standing mode of the spin-wave resonance having frequency ~ 4.7 GHz in Fig. 8). For example, for a quasisurface $n=0$ spin-wave mode propagating at the angle $\varphi=15^\circ$ to the in-plane bias magnetic field the hybridization with the $n=1$ mode happens at $k\sim 900$ cm^{-1} (see Fig. 8).

The input wire antenna (see 4 in Fig. 1) excited in our experimental Py film of the thickness $L=0.5$ μm SMSWs with $\varphi=90^\circ$ and $k\sim 15$ cm^{-1} , and the group velocity of these waves was $v_g=2\times 10^7$ cm/s . In the course of propagation these SMSWs excited (mostly due to the two-magnon scattering process) quasistanding ($v_g\sim 0$) BVMSWs with the same frequency but different wave number. It can be seen from Fig. 8 that the BVMSW mode, having the same frequency as the signal in our experiment ($f_k=f_s=4643$ MHz), corresponds to $\varphi\approx 10^\circ$ and has group velocity close to zero at $k\sim 3.5\times 10^3$ cm^{-1} . Due to the fact that SMSWs have a much smaller wave number ($k_{\text{SMSW}}\sim 15$ cm^{-1}) than BVMSW ($k_{\text{BVMSW}}\sim 3.5\times 10^3$ cm^{-1}) the interaction of SMSW with the wire input antenna (of the diameter $d=50$ μm) is much stronger. At the same time BVMSWs, because of their lower dissipation and weak interaction with antenna, have a substantially lower threshold of parametric instability under the influence of pumping and, therefore, a larger increment of parametric amplification by pumping.

These considerations allow us to identify the earlier introduced spin-wave groups SW_1 and SW_2 as SMSW and BVMSW, correspondingly. As for the third spin-wave group SW_3 , we identify it with short-wavelength plane spin waves, corresponding to higher-order ($n>1$) spin-wave modes of the Py film. These short-wavelength exchange-dominated spin waves are typically excited by parallel pumping at the threshold (see, e.g., Refs. 8 and 10) and, practically, do not interact with the input antenna due to the large magnitudes of their wave numbers. The spectra of these higher-order ($n>1$) spin-wave modes (i.e., modes having a larger value of the wave vector component $k_n=n\pi/L$ along the film thickness L) are, in general, similar to the spectra of the lower-order modes shown in Fig. 8, but their frequencies are shifted up by the exchange interaction. The frequencies of these modes for the vanishing in-plane wave vector $k\rightarrow 0$ are close to the frequencies of higher-order standing modes of the spin-wave resonance, having several nodes ($n>1$) in the distribution of their variable magnetization along the film thickness. The spectra of these higher-order modes for relatively large value of the in-plane wave vector k have minima due to the competition between the exchange and dipole-dipole interaction (see Ref. 14 for details), and the frequency magnitudes corresponding to these minima are increasing with the increase in the mode number n . For example, in the spectrum of our experimental Py film the minimum frequencies $f_{n\text{ min}}$ corresponding to spin-wave modes with different values of the mode number n are $f_{0\text{ min}}=1680$ MHz, $f_{1\text{ min}}=2648$ MHz, $f_{2\text{ min}}=3539$ MHz, $f_{3\text{ min}}=4471$ MHz, and

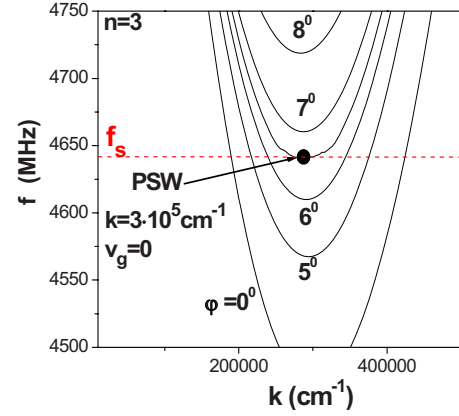


FIG. 9. (Color online) Dipole-exchange spin-wave spectrum for the $n=3$ thickness mode in a Py film calculated in the region near the bottom of the spectrum. The dashed horizontal line shows the position of the signal frequency equal to the half of the pumping frequency $f_p/2=f_s=4643$ MHz.

$f_{4\text{ min}}=5277$ MHz. At the same time, the values of the in-plane wave number k corresponding to these frequency minima remain almost the same: $k\sim(2-3)\times 10^5$ cm^{-1} .

From this analysis we can conclude that in our current experiment ($f_s=f_p/2=4.64$ GHz) the third group of spin waves SW_3 , participating in the parametric interaction with pumping and in the formation of the restored and delayed output signal, is the group of short-wavelength nonuniform plane spin waves with the “thickness” mode index $n\leq 3$ and $k\sim(2-3)\times 10^5$ cm^{-1} . These PSWs have the lowest threshold of parametric instability, the highest increment of parametric amplification by pumping, and the lowest coupling to the input antenna. It is the PSWs that determine the experimentally measured minimum threshold of spin-wave parametric instability (see Fig. 6) and only PSWs exist in the stationary regime of very long pumping pulses because they, in accordance with the S-theory,¹⁰ suppress all the other spin-wave groups after a long-enough interaction with pumping. The spectrum of the $n=3$ PSW mode having different propagation angles φ and calculated near the frequency minimum corresponding to $k=3\times 10^5$ cm^{-1} is presented in Fig. 9.

As it was pointed out earlier, the shape of the parametric instability threshold curve (or butterfly curve) in a Py film presented in the Fig. 6 is very different from the similar curve in a monocrystalline YIG film. One of the possible explanations of this difference is a much larger value of the FMR linewidth ΔH_k in Py compared to YIG. If the FMR linewidth ΔH_k in a magnetic film is larger than the frequency difference between the two neighboring standing modes of spin-wave resonance (i.e., modes with thickness indices n and $n+1$), the fine structure of the threshold curve that is easily seen in YIG will be smeared in Py. We believe, however, that it might be possible to see the fine structure of the threshold curve in thinner Py films, where the frequency interval between the different thickness spin-wave modes is larger than ΔH_k .¹⁶

The sharp increase in the parametric instability threshold, which is seen in Fig. 6 at $H_0\geq 325$ Oe, could be related to the fact that in this particular field interval the frequency of

the $n=3$ PSW mode becomes larger than the half of the pumping frequency or in other words the $n=3$ PSW mode falls out of the parametric resonance with pumping. It is clear from Fig. 9, where the spectrum of the $n=3$ PSW mode is shown in the region close to the half-frequency of the parametric pumping $f_p/2=4.64$ GHz, that at the bias field of $H_0=260$ Oe the pumping can effectively excite the $n=3$ PSW mode having the in-plane wave number $k=3 \times 10^5$ cm⁻¹ and propagating at the angle $\varphi=6.5^\circ$ relative to the in-plane bias magnetic field \mathbf{H}_0 . With the increase in the magnitude of the bias magnetic field by about 60 Oe all the $n=3$ PSW modes propagating in different directions increase their minimum frequencies f_k and, eventually, fall out of the parametric resonance condition $f_k=f_p/2$. Of course, in that case the $n=2$ PSW modes can be excited, but the parametric instability threshold for such modes will be much higher.

The experimentally observed resonance dependence of the output restored signal power on the bias magnetic field H_0 (see Fig. 6), also, finds a natural explanation in the framework of the above discussed qualitative model. Indeed, it is clear from Fig. 8 that the signal restoration effect is possible when the frequency $\omega_s=\omega_p/2$ of the input microwave signal lies between the FMR frequency of the Py film (4.61 GHz in the Fig. 8) and the frequency of the first ($n=1$) standing mode of the spin-wave resonance (4.7 GHz in the Fig. 8). That frequency interval of 90 MHz corresponds to the observed width $\delta H \sim 33$ Oe of the “resonancelike” curve of the restored signal shown in Fig. 6.

The rapid decrease in the restored signal clearly seen in Fig. 7 in the case when the pumping is switched on before the input signal (i.e., for $T_p < 0$) can be explained as follows. The exchange-dominated spin waves of the third group SW₃ (i.e., PSW), which start to be amplified from the thermal level as soon as pumping is on, reach such a large amplitude at the moment when the input signal is supplied, that they, through the phase mechanism of effective pumping renormalization,¹⁰ suppress the parametric amplification of the SMSW and BVMSW created by the signal. This suppression effect increases with the increase in the pumping power P_p and the absolute value of the time delay T_p between the pumping and signal pulses. According to our measurements, at $T_p=-20$ ns the amplitude of the PSW group becomes so high that the amplification of the signal-induced BVMSW and SMSW does not occur at all.

IV. CONCLUSION

In summary, we studied experimentally nonlinear interactions of several spin-wave groups with parametric microwave pumping in a thin Py film. It was found that the pulsed microwave signal of the frequency $f_s=4.7$ GHz supplied to the input wire antenna in an in-plane magnetized Py film excited surface magnetostatic spin waves (SMSWs) with the in-plane wave number $k \sim 15$ cm⁻¹. In the course of propagation and dissipation in the film these surface waves excited, through the mechanism of two-magnon scattering, a trail of quasistanding backward volume magnetostatic spin waves (BVMSWs) of the same frequency, but having a much

larger wave number of $k \sim 3.5 \times 10^3$ cm⁻¹. Both these wave groups were excited only near the input antenna.

Then, a powerful pulse of double-frequency ($f_p=2f_s$) microwave parametric pumping was supplied to the film through the open dielectric pumping resonator. The action of this parametric pumping leads to the amplification of the both signal-induced spin-wave groups and, also, to the excitation from the thermal level of the third spin-wave group of the same frequency, consisting of exchange-dominated short-wavelength ($k=3 \times 10^5$ cm⁻¹) plane spin waves, which have the strongest coupling to the parametric pumping.

The nonlinear interactions between these three spin-wave group and their mutual interaction with pumping determine the profile of the restored and delayed output microwave signal which appears at the input antenna after the pumping is switched on. The time delays of the output pulse experimentally measured in a Py film exceeded 100 ns. The amplitude, the duration, and the time delay of the output pulse could be controlled by the parameters (power and duration) of the signal and the pumping pulses, and the relative delay between them.

It was found that the process of pumping-induced microwave signal restoration takes place only in the input signal supplied to the film in an active time interval (namely, several tens of nanoseconds before the pumping is switched on) and that the amplitude of the restored signal has a “resonancelike” dependence on the magnitude of the in-plane bias magnetic field.¹⁶

Measuring the exponential decay of the trailing edge of the output restored pulse we were able to experimentally determine the intrinsic relaxation time of spin waves in a Py film. This relaxation time turned out to be 10–12 ns, which is almost five times larger than the spin-wave relaxation time, determined from the measurements of the parametric instability threshold in the same film. It was, also, found that under the influence of parametric pumping it is possible to increase the spin-wave relaxation time to 200 ns, which might be very important for the development of active microwave signal processing devices based of Py films.

It should be noted that the above presented investigations of nonlinear properties of spin waves in *metallic* films are of a considerable general interest since the increasing number of research groups study Py and other ferromagnetic metals as media for spin-wave propagation^{17–23} and as a material of choice for microwave signal processing devices.²⁴ Experimental methods based on nonlinear spin-wave phenomena described in this work can be useful for the precise experimental determination of parameters of metallic magnetic films. In particular, the method of measurement of dissipation rate of a parametrically restored signal (see Figs. 3 and 5) can be used for the determination of relaxation times of spin waves in metallic films used in passive microwave signal processing devices²⁴ and in active current-driven spin-torque nano-oscillators.²⁵

Also, the results of our current work and our previous paper³ allow us to make several general statements about the development of wave instability under the influence of parametric pumping. In the case when the pumping is continuous it excites one spin-wave group having the minimum parametric threshold. In contrast, in the case of a pulsed pumping

(i.e., in a transitional regime), due to the action of external signals and influence of linear two-magnon interaction between spin waves, pumping could excite simultaneously several spin-wave groups and, in particular, spin-wave groups having effective relaxation time that is substantially larger than the typical wave relaxation time in a passive (no pumping) regime. This transitional behavior of parametric spin waves was observed in both dielectric³ and metallic (this work) magnetic films, where static magnetizations, spin-wave relaxation times, and efficiencies of two-magnon scattering were drastically different [e.g., spin-wave relaxation times in metallic films are 2 orders of magnitude shorter than in monocrystalline ferrite films (YIG)].

This similarity of transitional parametric wave processes in such different media allows us to believe that the observed transitional parametric phenomena are rather general and that similar scenarios of parametric instability development can be expected in plasma physics, nonlinear optics, and nonlinear acoustics in the case of pulsed pumping.

ACKNOWLEDGMENTS

This work was supported by the Ukrainian Fund for Fundamental Research under Contract No. 25.2/009, by the MURI grant from the U.S. Army Research Office under Contract No. W911NF-04-1-0247, and by the Oakland University Foundation.

-
- ¹G. A. Melkov, A. A. Serga, V. S. Tiberkevich, A. N. Oliynyk, and A. N. Slavin, *Phys. Rev. Lett.* **84**, 3438 (2000).
- ²G. A. Melkov, Yu. V. Kobljanskyj, A. A. Serga, V. S. Tiberkevich, and A. N. Slavin, *Phys. Rev. Lett.* **86**, 4918 (2001).
- ³A. A. Serga, A. V. Chumak, A. Andre, G. A. Melkov, A. N. Slavin, S. O. Demokritov, and B. Hillebrands, *Phys. Rev. Lett.* **99**, 227202 (2007).
- ⁴Yu. V. Kobljanskyj, G. A. Melkov, V. M. Pan, V. S. Tiberkevich, and A. N. Slavin, *IEEE Trans. Magn.* **38**, 3102 (2002).
- ⁵Yu. V. Kobljanskyj, G. A. Melkov, V. S. Tiberkevich, V. I. Vasyuchka, and A. N. Slavin, *J. Appl. Phys.* **93**, 8594 (2003).
- ⁶G. A. Melkov, Yu. V. Kobljanskyj, V. I. Vasyuchka, A. V. Chumak, and A. N. Slavin, *IEEE Trans. Magn.* **40**, 2814 (2004).
- ⁷G. A. Melkov, V. I. Vasyuchka, V. A. Moiseienko, and A. N. Slavin, Abstracts of the International Magnetism Conference INTERMAG-08, Madrid, Spain, May 2008 (unpublished), Abstract No. BG-04.
- ⁸A. G. Gurevich and G. A. Melkov, *Magnetization Oscillations and Waves* (CRC, New York, 1996).
- ⁹P. Krivosik, K. Srinivasan, H. M. Olson, and C. E. Patton, Abstracts of INTERMAG-06 Conference, San Diego, California, 8–12 May 2006 (unpublished), Abstract No. BA-06.
- ¹⁰V. S. L'vov, *Wave Turbulence under Parametric Excitations* (Springer-Verlag, Berlin, 1994).
- ¹¹Yu. V. Kobljanskyj, V. S. Tiberkevich, A. V. Chumak, V. I. Vasyuchka, G. A. Melkov, and A. N. Slavin, *J. Magn. Magn. Mater.* **272–276**, 991 (2004).
- ¹²G. A. Melkov, A. A. Serga, V. S. Tiberkevich, A. N. Oliynyk, A. V. Bagada, and A. N. Slavin, *J. Exp. Theor. Phys.* **89**, 1189 (1999).
- ¹³E. Schlömann, J. J. Green, and U. Milano, *J. Appl. Phys.* **31**, S386 (1960).
- ¹⁴B. A. Kalinikos, N. G. Kovshikov, and N. V. Kozhus, *Sov. Phys. Solid State* **27**, 2794 (1985).
- ¹⁵B. A. Kalinikos and A. N. Slavin, *J. Phys. C* **19**, 7013 (1986).
- ¹⁶J. B. Comly and R. V. Jones, *J. Appl. Phys.* **36**, 1201 (1965).
- ¹⁷M. Bailleul, D. Olligs, C. Fermon, and S. O. Demokritov, *Europhys. Lett.* **56**, 741 (2001).
- ¹⁸T. J. Silva, M. R. Pufall, and P. Kabos, *J. Appl. Phys.* **91**, 1066 (2002).
- ¹⁹M. Covington, T. M. Crawford, and G. J. Parker, *Phys. Rev. Lett.* **89**, 237202 (2002).
- ²⁰M. Bailleul, D. Olligs, and C. Fermon, *Appl. Phys. Lett.* **83**, 972 (2003).
- ²¹M. L. Schneider, Th. Gerrits, A. B. Kos, and T. J. Silva, *Appl. Phys. Lett.* **87**, 072509 (2005).
- ²²Z. Liu, F. Giesen, X. Zhu, R. D. Sydora, and M. R. Freeman, *Phys. Rev. Lett.* **98**, 087201 (2007).
- ²³K. Perzlmaier, G. Woltersdorf, and C. H. Back, *Phys. Rev. B* **77**, 054425 (2008).
- ²⁴Y. Khivintsev, R. E. Camley, and Z. Celinski, Abstracts of the 2008 Conference on Magnetism and Magnetic Materials (MMM-2008), Austin, Texas, November 2008, Abstract No. BF-05, p. 98.
- ²⁵T. J. Silva and W. H. Rippard, *J. Magn. Magn. Mater.* **320**, 1260 (2008).